Polymer Chemistry

Accepted Manuscript

ROYAL SOCIETY OF CHEMISTRY

www.rsc.org/polymers

Cite this: DOI: 10.1039/c0xx00000x

www.rsc.org/xxxxxx

ARTICLE TYPE

Cyclodextrin-calixarene co-polymers as a new class of nanosponges

Paolo Lo Meo,*[a] Giuseppe Lazzara,[b] Leonarda Liotta,[c] Serena Riela[a] and Renato Noto*[a]

Received (in XXX, XXX) Xth XXXXXXXXX 20XX, Accepted Xth XXXXXXXXX 20XX
DOI: 10.1039/b000000x

Hyper-reticulated co-polymers jointly formed by cyclodextrin and calixarene units, which can be considered as a new class of nanosponges, were easily obtained by means of a click chemistry approach. In particular, we succeeded in preparing our materials by exploiting the copper-catalyzed 1,3-dipolar cycloaddition (CuAAC) reaction between the *heptakis*-(6-deoxy)-(6-azido)-β-cyclodextrin and the (5,11,17,23-tetra-*tert*-butyl)-(25,26,27,28-tetra-propargyloxy)-calix-[4]-arene, mixed in different proportions. These materials were fully characterized by means of combined FT-IR, thermogravimetric, ^{13}C {^{1}H} CP-MAS NMR and nitrogen adsorption/desorption techniques. In particular, ^{13}C {^{1}H} CP-MAS spectra allowed us to perform a quantitative analysis of the co-polymers obtained. Tests on their possible sequestering abilities towards some organic molecules, in particular nitroarenes and commercial dyes chosen as suitable pollutant or drug models, were successfully carried out. Results obtained point out that absorption abilities seem affected by polymer composition and porosity as well.

Introduction

Nanosponges constitute a new class of hyper-reticulated polymeric materials, able to absorb or release in a controlled way different organic species.[1] These materials, which can be formed by polymerizing a potential supramolecular host, have found various applications in several technological fields, spanning from drug carrier systems[1,2] to agrochemicals,[3] gas storage[4] and environment remediation.[5] In particular, the most known and used nanosponges have been obtained from native cyclodextrins (**CD**s), randomly cross-linked by reacting them with suitable electrophilic link-making reagents, such as epichlorohydrin,[6] carbonic acid esters,[7] carbonyldiimidazole[8] or diisocyanates.[9,10] The reaction, of course, exploits the nucleophilic reactivity of both primary and secondary hydroxyl groups of the **CD** units.

The usefulness and potential applications of these materials are obviously bound to the intrinsic affinity of the host monomer, *i.e.* the **CD** unit for instance, towards given target guest molecules. Therefore, we may reason that the inclusion or release properties of a nanosponge might undergo significant modification and improvement by exploiting the co-polymerization of two different hosts having somehow complementary binding abilities. Under this light, Calix-[*n*]-arenes (**C*n***s) appear as ideal candidates for co-polymerization with **CD**s. Indeed, **C*n***s are wholly synthetic macrocyles, which can be easily prepared and chemically modified through well assessed and relatively simple synthetic procedures.[11] Although less systematically investigated as compared to **CD**s, **C*n***s can effectively bind small and medium-sized organic molecules, as well as organic or inorganic ionic species.[12,13] The microscopic interactions involved in host-guest binding for the two classes of macrocycles are deeply different. For **CD**s a subtle interplay takes place between hydrophobic, dipolar and hydrogen bond interactions, conformational restraints and solvation effects.[14-16] For **C*n***s, on the other hand, an important role is played by the π-π or the cation-π[13,17] interactions with the arene cavity; however, interactions between the guest and possible ancillary donor groups suitably linked to the **C*n*** scaffold[12,13,18] often assume a paramount importance.

There are some recent reports describing the synthesis of joined supramolecular hosts[19] obtained *via* a typical "click chemistry" approach, by exploiting the well known copper catalyzed azide-alkyne 1,3-dipolar cycloaddition (CuAAC reaction).[20] We reasoned that the same approach could be extended to the synthesis of mixed **CD**/**C*n*** co-polymers. In the present paper we describe the preparation, the characterization and a first study on the binding properties of a set of **CD**/**C*n*** co-polymeric materials obtained by reacting the easily accessible *heptakis*-(6-deoxy)-(6-azido)-β-**CD** **1**[21] and (5,11,17,23-tetra-*tert*-butyl)-(25,26,27,28-tetra-propargyl-oxy)-calix-[4]-arene **2**[22] (Scheme 1). The obtained materials were characterized by means of combined FT-IR, thermogravimetry, solid state NMR and N_2 absorption/desorption techniques. Moreover, we performed some tests on their potential sequestering abilities towards some organic molecules chosen as model pollutants or drugs.

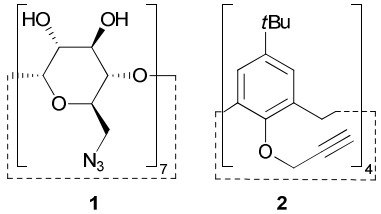

1 **2**

Scheme 1 Structures of the co-monomers **1** and **2**.

Results and Discussion

Synthesis of the materials

The starting synthons **1** and **2** can be prepared by means of well known procedures (Scheme 2). In particular, the azido-β-**CD 1** is obtained in excellent yields (ca. 95 %) *via* nucleophilic displacement from the *heptakis*-(6-deoxy)-(6-iodo)-β-**CD**,[23] which in turn is prepared from native β-**CD** by reaction with the Vilsmeyer-Haack reagent (iodine and triphenylphosphine). On the other hand, the propargyl-**C*n* 2** can be obtained in fair yields (ca 40 %) by reaction between the (5,11,17,23-tetra-*tert*-butyl)-calix[4]arene and propargyl bromide (Scheme 2).

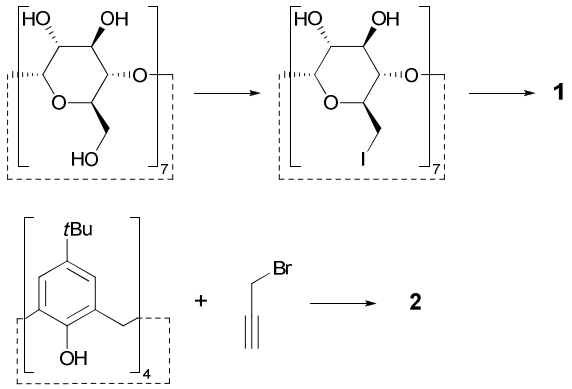

Scheme 2 Synthesis of synthons **1** and **2**.

Before attempting the CuAAC coupling reaction between **1** and **2**, we carried out a preliminary search for the most suitable operational conditions. For this purpose we studied the reaction between **1** and (*p-tert*-butyl)-phenyl-propargyl ether **3** to afford the *heptakis*-(6-deoxy)-(6-{[4-(*p-tert*-butylphenoxy)methyl]-1,2,3-triazol-1-yl})-β-**CD 4** (Scheme 3). It is worth noting, indeed, that **4** served as a suitable reference compound for the subsequent characterization of the polymeric materials. The reaction was satisfactorily carried out in DMSO for 18 h at 70 °C, using a 5 % mole amount of cupric sulphate/sodium ascorbate as the catalyst, and resulted in a 90 % yield. We found out that the correct choice of the solvent is quite important. As a matter of fact, the reaction gave very poor yields when performed in water, butanol, DMF or their mixtures (the other conditions being equal), which are all typical solvents used for this kind of reaction.

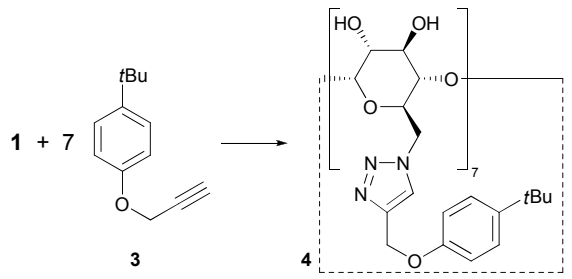

Scheme 3 Synthesis of the model compound **4**.

For the synthesis of the co-polymers, we allowed to react the starting synthons **1** and **2** mixed in different proportions. As a matter of fact, we were interested in obtaining materials with different compositions, having an excess of unreacted azide or alkyne groups able to undergo further transformations. Indeed, the -N_3 group may be easily reduced to -NH_2 under the Staudinger reaction conditions[24] (triphenylphosphine and base), whereas the -C≡CH group may be either oxidized or reduced. The amounts of reactants and their combination equivalent ratios are summarized in Table 1, together with the mass yields obtained. For the sake of clarity, reactants amounts were calculated according to the formal (equivalent) masses of the functionalized subunits of the co-monomers, *i.e.* the azido-glucose residue (187 Da, corresponding to $C_6H_9N_3O_4$) and the *tert*-butyl-propargyloxy-phenyl-methylene residue (200 Da, corresponding to $C_{14}H_{16}O$). We chose six different equivalent ratios, namely 4:1, 2:1, 1:1, 1:2, 1:3.5 and 1:7; the corresponding products are identified as **P1-P6** respectively. Noticeably, the last ratio was chosen in such a way to exceed the minimum stoicheiometric conditions for the formation of an individual compound constituted by a **CD** surrounded by seven **C*n*** units. A possible pictorial representation of the random co-polymeric structure is provided in Fig. 1.

Table 1 Reactant ratios and mass yields for polymers **P1-P6**.

Reactants	**P1**	**P2**	**P3**	**P4**	**P5**	**P6**
1 (meq.)	1.0	1.0	0.5	0.25	0.143	0.143
(mg)	187.0	187.0	93.5	46.7	26.7	26.7
2 (meq.)	0.25	0.5	0.5	0.5	0.5	1.0
(mg)	50.0	100.0	100.0	100.0	100.0	200.0
1:**2** eq. ratio	4 : 1	2 : 1	1 : 1	1 : 2	1 : 3.5	1 : 7
yield (mg)	170.6	243.9	185.8	139.3	101.6	172.3
(%)	(72)	(85)	(96)	(95)	(80)	(76)

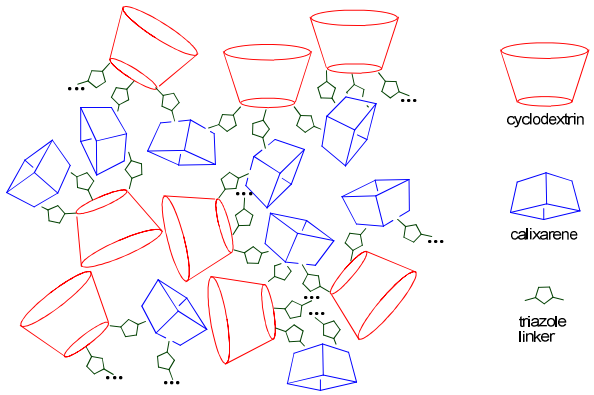

Fig. 1 Possible depiction of the random co-polymer structure.

In a typical preparation the proper amounts of reactants and catalyst were mixed in a dark vial, dissolved/suspended in DMSO, and allowed to react for 18 hours at 70 °C. Then, the polymeric material was isolated by subsequent washings with water, methanol and diethyl ether, in order to remove the DMSO, the catalyst and the residual unreacted reagents. Three different washing protocols were set up, changing the order by which the solvents were used (see Experimental). However, we verified that the particular protocol used did not significantly affect the mass yields in the obtained products; therefore, only the average results were reported in Table 1 (we also verified that the washing protocol did not affect any of the results from subsequent FT-IR or TGA analyses). Isolated mass yields follow a bell-shaped trend on changing the reactant combination ratio, with the largest value found for the ideal 1:1 azide/alkyne equivalent ratio (*i.e.* product **P3**). The materials obtained were not subjected to any further purification before subsequent investigations.

Characterization of the materials

FT-IR - Fourier-Transform Infrared spectroscopy (FT-IR) is undoubtedly the most simple and immediate technique by which nanosponge materials can be characterized, and it has been widely used for this purpose.[8,25] We performed a preliminary characterization of the starting synthons **1** and **2**, as well as of the alkyne ether **3** and the model product **4**, in order to identify the diagnostic signals attributable to the **CD** and **C*n*** scaffolds and to the resulting triazole ring. The most significant features which can be recognized in the spectrum of **1** (nujol mull) are the sharp band at 2110 cm^{-1} for the $-N_3$ stretching and the scaffold fingerprints at 1295, 1157, 1078 and 1051 cm^{-1}. On the other hand, **2** shows a weak band centered at 2119 cm^{-1} (-C≡CH stretching), aromatic ring stretching bands at 1587 and 1479 cm^{-1}, and sharp scaffold fingerprints at 1363, 1191, 1118, 1109, 1008 and 994 cm^{-1}. Similar bands can be easily identified in the spectrum of **3** (2122, 1610, 1583, 1364, 1298, 1264, 1225, 1185, 1032, and 829 cm^{-1}). The reference triazolyl-β-**CD 4** clearly shows the almost complete disappearance of the azide signal (the superimposed spectra of compounds **1**, **3** and **4** in the ranges 2300-2000 cm^{-1} and 1700-800 cm^{-1} are shown in Fig. 2). Moreover, **4** shows three bands in its fingerprints region (1154, 1077 and 1048 cm^{-1}), which can be easily attributed to the **CD** scaffold, together with three further signals (1295, 1185 and 829 cm^{-1}) which are clearly fingerprints of **3**. Finally, there are two further bands at 1244 and 1018 cm^{-1} which are not comparable to any of the signals of the reactants, and thus can be attributed to vibration modes of the triazole rings.

Having gained this information, we could pass to analyze the spectra of materials **P1-P6** (see Fig. S1-S6 in Supporting). As a representative example, Fig. 3 shows in superimposition the spectra of the co-monomers **1** and **2** and the material **P3**. For the latter one, careful examination of the fingerprint region shows the simultaneous presence of signals attributable to both the **CD** (1295, 1156, 1078, 1049 cm^{-1}) and the **C*n*** (1364, 1189 and 1115 cm^{-1}) scaffolds. Moreover, it is possible to identify a band at 1239 cm^{-1} and a shoulder at ca. 1015 cm^{-1}, accounting for the formation of the triazole ring, which provide unambiguous confirmation that the coupling process between the co-monomers actually occurred. It is interesting to notice that a little signal at 2119 cm^{-1} is still present in the spectrum, indicating that not all the reactive functional groups in the starting reactants actually happened to react. This may be a consequence of the hyper-reticulated nature of the co-polymers obtained. Steric hindrances and strains, indeed, might prevent some of the reacting groups to achieve the minimum arrangement requirements needed for the cycloaddition process to occur.

General inspection of the spectra of the other materials confirms the presence of the same bands as in the spectrum of **P3**, although the relative intensities of the signals change consistently with the reactant ratio used in the synthesis. Comparison between the superimposed spectra of materials **P1**, **P3** and **P6** (chosen as a suitable example, Fig. 4) clearly shows the regular increase in intensity of the **C*n*** fingerprints (1480, 1364, 1189 and 1115 cm^{-1}) and the concomitant decrease of the **CD** fingerprints (1156, 1078 and 1049 cm^{-1}). The triazole signal at 1239 cm^{-1} can be clearly identified in the spectrum of **P1**, but is hardly visible in **P6**, whereas the shoulder at 1015 cm^{-1} is much more apparent in the spectrum of **P3** than in **P1**. The latter findings can be easily explained considering that the 1:1 equivalent reactant ratio used for the synthesis of **P3** provides the conditions for the most extensive occurrence of the triazole ring formation. Finally, the spectra of **P1** and **P2** show remarkable signals for the $-N_3$ stretching at 2110 cm^{-1}, due to the fact that the azido-β-**CD 1** is the component in excess for their preparation. The relative intensity of the signal, compared to the intensity of the **CD** fingerprint at 1049 cm^{-1} assumed as a suitable reference, regularly decreases along the series **P1** > **P2** > **P3**, consistently with the composition of the reaction mixture. On the other hand, products **P5** and **P6** show a tiny signal at ca. 2120 cm^{-1}, which accounts for presence of the unreacted alkyne component in excess.

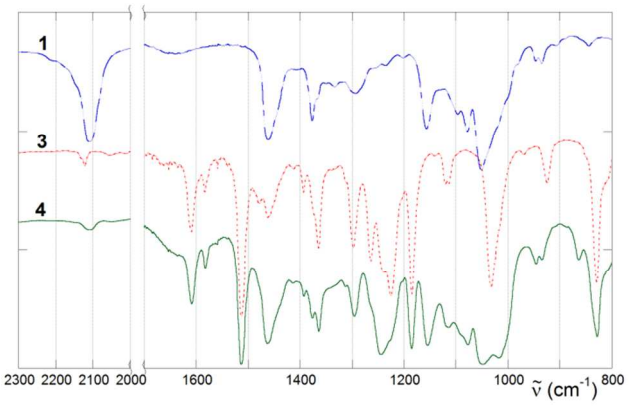

Fig. 2 FT-IR spectra of compounds **1**, **3** and **4**.

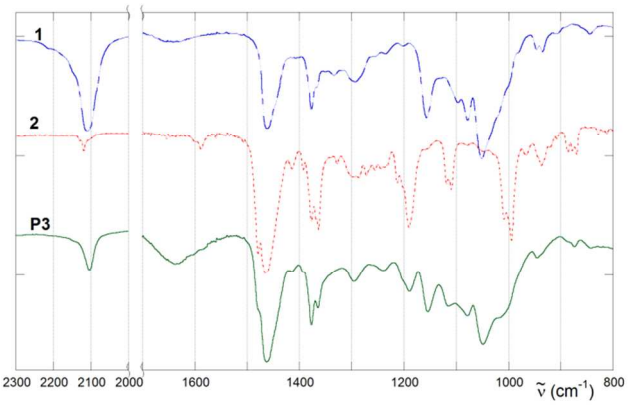

Fig. 3 FT-IR spectra of compounds **1** and **4** and material **P3**.

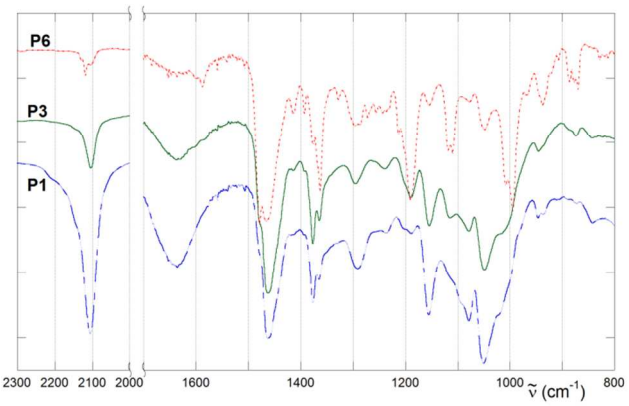

Fig. 4 FT-IR spectra of materials **P1**, **P3** and **P6**.

TGA and DTG – Thermogravimetric (TGA) and Differential Thermogravimetric (DTG) Analysis techniques provide with an important piece of information on the thermal stability of materials in general. In some cases these techniques have allowed to achieve semi-quantitative (or even quantitative)[26] information on composition. Furthermore, thermal stability is an important requirement in view of any possible application of nanosponge materials. Similarly as to the FT-IR study, we performed a preliminary analysis of the starting synthons **1** and **2** and the reference product **4** (the normalized thermograms and relevant differential thermograms are shown in Fig. 5 and 6 respectively). Both the azido-β-**CD 1** and the triazolyl-β-**CD 4** show one sharp degradation step, centered at 222 °C and 304 °C respectively, accounting for nearly a 50 % mass loss. Thus, the occurrence of the cycloaddition reaction improves the thermal stability of the **CD** scaffold, owing to the larger stability of the aromatic triazole moiety with respect to the simple azide group. Subsequent heating up to 900 °C results in the almost complete degradation of **4**, whereas under the same conditions a ca. 20 % in weight residue is still present for **1**. By contrast, the propargyloxy-**C*n*** **2** shows a more extensive thermal stability, with a much smoother degradation trace. Deconvolution analysis of the DTG curve reveals that this consists of two superimposed decomposition steps centered at 422 °C and 481 °C respectively, accounting for an overall 60 % mass loss, whereas subsequent heating up to 900 °C results in a further 20 % ca. mass loss.

Analysis of the normalized TGA and DTG curves for materials **P1**-**P6** (Figures 7 and 8) is very interesting. Starting from the former one, prepared with the largest amount of **1**, we can notice the presence of a main decomposition peak in the DTG curve centered at 218 °C, followed by a secondary one at 310 °C. These peaks may easily be attributed to the thermal decomposition of the unreacted azido-glucose units and the triazole-glucose units present in the co-polymer respectively. In the DTG curve of **P2** the second peak becomes the highest one, in agreement with the fact that, having prepared the co-polymer with a larger amount of the alkyne component, a lesser amount of unreacted -N_3 groups and a larger amount of triazole linkers must be present in the material. Accordingly, in the curve of **P3** the first peak appears very small (and shifted up to 234 °C), whereas the second one reaches its maximum height; moreover, a third peak appears at 468 °C, which can be attributed to the thermal decomposition of the **C*n*** scaffold. Noticeably, the intensity trend for the first peak is perfectly consistent with the one mentioned previously for the azide stretching band observed in the FT-IR spectra. For **P4** and **P5** the first peak has almost disappeared and the second one progressively decreases in intensity, whereas the third one increases. Finally, **P6** shows three largely overlapped but distinct peaks at 254 °C, 409 °C and 465 °C.

On the whole, thermogravimetric data provide a much more convincing evidence of the presence of the triazole ring linkers suggested by FT-IR spectra, confirming the actual occurrence of the "click" reaction and the formation of the co-polymer network. Moreover, DTG curves confirm that the largest relative amount of triazole units can be found, and therefore that the most extensive degree of cross-linking is achieved, as the reactants mixture approaches the ideal 1:1 eq. composition. However, owing to the large residual masses present at 900 °C and to the

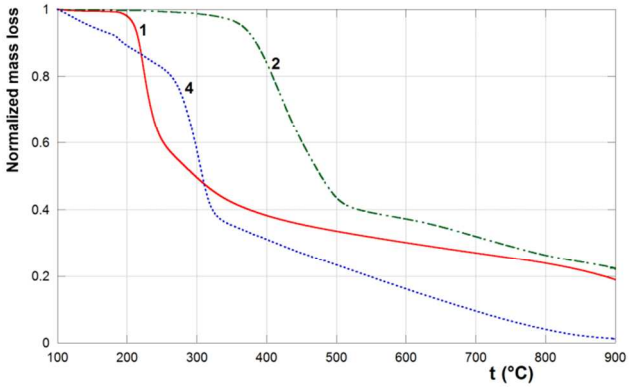

Fig. 5 TGA curves for compounds **1**, **2** and **4**

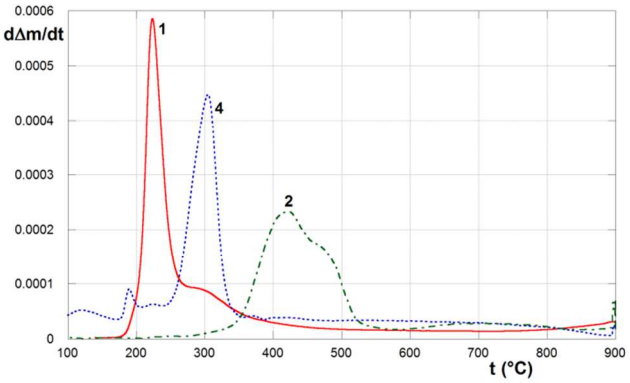

Fig. 6 DTG curves for compounds **1**, **2** and **4**

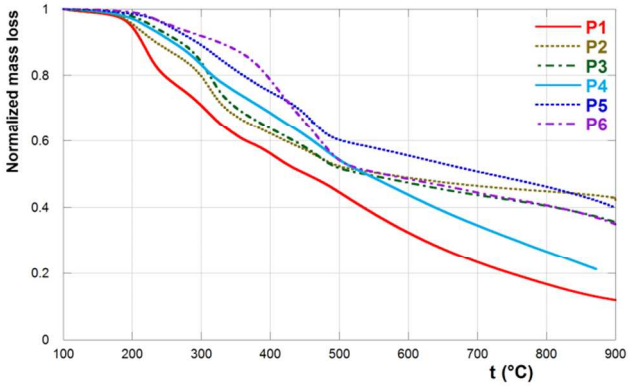

Fig. 7 TGA curves for materials **P1**-**P6**

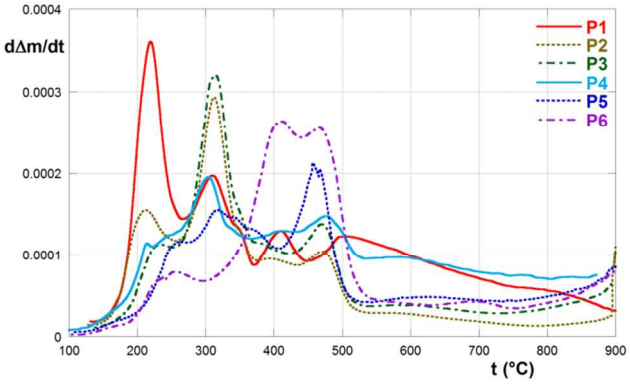

Fig. 8 DTG curves for materials **P1**-**P6**

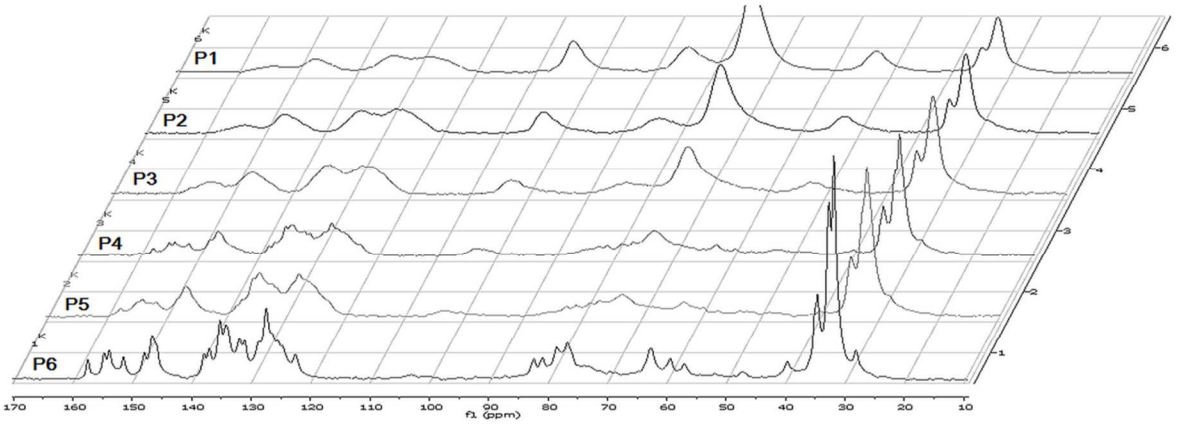

Fig. 9 ^{13}C {^{1}H} CP-MAS spectra of materials **P1**-**P6**

complexity of the DTG curves, we were not able to perform a reliable deconvolution analysis, in order to get at least a semi-quantitative estimation of the actual composition of the products obtained.

CP-MAS NMR – Cross Polarization Magic Angle Spinning (CP-MAS) NMR has gained increasing importance in the study of solid state or soft materials. In particular, the Cross Polarization (CP) technique[27] allows the registration of the spectra of dilute nuclei such as ^{13}C in the solid state in reasonable times. Therefore, it is a particularly versatile and informative tool for the study of organic polymeric materials such as our ones, which show no appreciable solubility in any common solvent. At the best of our knowledge, however, this technique has never been employed in the study of nanosponge materials.

The superimposed ^{13}C {^{1}H} CP-MAS NMR spectra of materials **P1**-**P6** are synoptically shown in Fig. 9. Spectra, in general, show large signals or clusters of signals corresponding to C atoms in different chemical environments. Attributions (Fig. 10) can be done keeping into account the spectra of compounds **1**, **2** and **4** recorded in solution as suitable references.

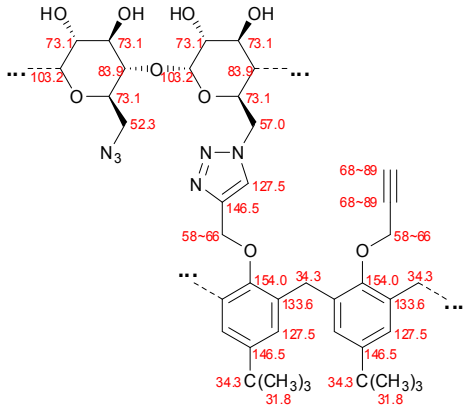

Fig. 10 Attributions of the ^{13}C resonances for materials **P1**-**P6**

The spectrum of **P6** shows intense signals which can be unambiguously attributed to the **C*n*** monomers, in particular: *i*) a cluster of five signals in the range 22~43 ppm for the *tert*-butyl groups and the methylene bridges of the **C*n*** scaffold; *ii*) four distinct clusters in the range 120~160 ppm for the aromatic and heteroaromatic C atoms. The spectrum shows also two broad clusters in the ranges 58~66 ppm and 68~89 ppm, which can be collectively attributed to the **C*n*** methylenoxy and the unreacted alkyne groups overlapped with the **CD** carbon atoms; finally, a weak signal is present at 103.0 ppm, attributable to the **CD** monomers too. As a matter of fact, at the other composition extreme, the spectrum of **P1** shows four large bands centered at 52.3, 73.1, 83.9 and 103.2 ppm. The signals at 52.3 and 103.2 can be confidently assigned to the C(6) and C(1) atoms of the **CD** scaffold respectively, whereas the other two signals fall in the typical range for the C(2-5) atoms of the **CD**, although it is reasonable to assume that they possibly cover the methylenoxy **C*n*** signals. Owing to the fact that the **CD** co-monomer was present in large excess in the reaction mixture, we can assume that nearly no unreacted alkyne group is present, and that most of the **CD**-C(6) atoms are bound to unreacted azide groups. Therefore, by comparison with the spectrum in solution of **1**, the resonance at 52.3 ppm can be unambiguously assigned to these azide-bound **CD**-C(6) atoms. Similarly, comparison with the spectrum of **4** suggests that the triazole-bound **CD**-C(6) atoms in the product **P6** may be tentatively identified with a tiny signal centered at 57.0 ppm. The spectrum of **P1**, of course, shows also the signals for the **C*n*** co-monomers, although a significant loss in resolution is clearly apparent. In particular, we can notice a broad band centered at 31.8 ppm overlapped with a smaller one at 34.3 ppm for the aliphatic carbons (methylenoxy excluded), in place of the five sharper signals at 22~43 ppm mentioned previously. Similarly, we can also notice four broad, partly overlapped bands for the aromatic carbons, centered at 127.5, 133.6, 146.5 and 154.0 ppm respectively, in place of the four corresponding clusters found for **P6**.

Comparison between the spectra of the different products clearly shows, on going from **P1** to **P6**, a gradual change in the relative intensities and in the resolution of the signals attributable to the **CD**s and the **C*n***s respectively. Indeed, a particularly intriguing feature of the CP-MAS technique is the possibility to gain quantitative information from signal integration of the ^{13}C spectrum, under the hypothesis that the effects of H-C cross polarization operate homogeneously for all the C atoms present in the sample.[28] Such an assumption, of course, cannot be done *a priori*; nevertheless, integration analysis of the spectra allowed us to obtain very interesting results. Starting from material **P1**, due

to the presence of a large excess of the azide component, we may reasonably assume that nearly all the alkyne groups of the C***n*** co-monomers have actually undergone the coupling reaction. Therefore, their C atoms have been engaged in the triazole ring formation, and consequently have become aromatic in nature. Thus, a 5:8 ratio should be observed on comparing the cumulative integrals of the C***n*** aliphatic signals centered at 31.8 and 34.3 ppm and the aromatic signals in the 120~160 ppm range. We actually found a 5:7.4 ratio, which seems in acceptable agreement with the expected one. Furthermore, assumed the C***n*** aliphatic signals as an internal standard integrating for five carbons, it is very interesting to notice that the aforementioned ratio decreases constantly along the spectra set, passing to 5:7.1 for **P2**, 5:7.0 for **P3**, 5:6.3 for **P4**, 5:6.2 for **P5** and 5:5.9 for **P6** (in the latter case we are referring, of course, to the cluster in the range 22~43 ppm). This trend perfectly agrees with the fact that, on increasing the amount of the C***n*** component in the reaction mixture, an increasing fraction of alkyne groups remains unreacted in the final material, in particular when **2** is the reactant in excess. Noticeably, the integration ratio shows a significant drop on passing from **P3** to **P4**, *i.e.* on passing from a 1:1 to a 1:2 azide/alkyne equivalent ratio. So, assuming the 5:7.4 ratio found for **P1** as a suitable scaling factor, the result found for **P3** indicates (see Supporting for mathematical details) that a 78% ca. of alkyne groups have been actually engaged in the triazole ring formation reaction. Considering the 1:1 equivalent ratio used in its synthesis, this in turn means that the same amount of azide groups has reacted as well, and therefore a 22% of unreacted azide should be still present in the material. The latter result is in perfect agreement with the FT-IR and DTG evidences discussed previously. Following this line, we can estimate that ca. 84% of alkyne groups have actually reacted in **P2**, 43% in **P4**, 35% in **P5**, and 19% in **P6.**

Considering now product **P3**, owing to the fact that it is obtained in almost quantitative mass yield (but for the minor unavoidable losses occurring during the work-up procedure), we may reasonably assume that its final co-monomer composition is the same as in the corresponding reaction mixture. Therefore, the 1:1 equivalent ratio between the functionalized co-monomer subunits (azido-glucose or *tert*-butyl-propargyloxy-phenyl-methylene) must have been maintained in the material. As a consequence, on comparing the aliphatic C***n*** signals at 31.8 and 34.3 ppm with the **CD**-C(1) signal at 103.0 ppm chosen as suitable references, a 5:1 integration ratio should be expected. The result we actually found, *i.e.* 5:1.07, appears in quite satisfactory agreement. So, we can use it as a scaling factor in order to get a quantitative estimation of the real equivalent ratio occurring in each material, and correspondingly of the actual co-monomer composition (the latter one can be simply calculated multiplying by 4/7 the equivalent ratio found). Relevant results are summarized in Table 2. As we can see, data indicate that product **P4** has a composition almost identical to the one expected on the grounds of the equivalent ratio used. On the other hand, for the other products there are significant deviations from the composition expected, indicating that part of the reactant in excess has not undergone the coupling reaction and, consequently, has been lost during the work-up. Therefore, the relevant mass losses can be calculated accordingly, and appear in acceptable agreement with the

Table 2 Signal integration analysis for products **P1-P6**

	P1	**P2**	**P3**	**P4**	**P5**	**P6**
integral for **CD**-C(1)[a]	3.48	1.75	1.07	0.53	0.38	[b]
1:**2** eq. ratio[c] experimental (in reaction)	3.3:1 (4:1)	1.6:1 (2:1)	1:1[d] (1:1)	1:2.0 (1:2)	1:2.8 (1:3.5)	1:5.3[e] (1:7)
actual **CD**/C***n*** mole ratio	1.89	0.91	0.57	0.29	0.20	0.11
% mass loss predicted (experimental)	14 (28)	13 (15)	0 (4)	0 (5)	16 (20)	22 (24)

[a] Cumulative integration of the aliphatic C***n*** signals set equal to 5 as the standard; data given within a ± 3% indetermination. [b] Signal too weak for a reliable integration. [c] To be intended as the ratio between the amounts of functionalized subunits of the co-monomers. [d] Set as the standard. [e] Calculated by comparing the cumulative integrals for the signal clusters at 22~43 ppm and 120~160 ppm (see text).

experimental yields. Material **P1** presents on average nearly two **CD** units per C***n*** unit, whereas **P5** has five C***n*** units per **CD**. For product **P6**, it must be mentioned that the **CD**-C(1) signal at ca. 103 ppm is too weak to allow a reliable integration. However, keeping into account the aforementioned estimation that only 19% of alkyne groups have actually reacted, an azide/alkyne equivalent ratio can be calculated for the product composition as large as 1:5.3, corresponding to an actual **CD**/C***n*** mole ratio as large as 0.11. The latter result is intriguing, because it accounts for the presence in the structure of ca. nine C***n*** units on average per **CD**. Thus, the amount of C***n*** apparently exceeds the one needed for the formation of an individual species constituted by a single **CD** unit bound to seven C***n***s. Assumed that the polymeric network has been actually formed, as accounted for by thermogravimetric evidences, this means that a significant amount of unreacted **2** should have remained entrapped within the reticulated polymer structure.

SSA/Porosimetry – Finally, Specific Surface Area (SSA) measurements and pore texture analyses were performed, in order to get further information on the microscopic structure of the materials. Nitrogen adsorption/desorption is the most widely used technique to determine solid surface area and to study the porous structure, and it has been occasionally applied to cyclodextrin-based cross-linked polymers too.[10,29] Therefore, we employed it in particular in order to characterize materials **P1-P4**. The relevant textural parameters in terms of specific surface area (obtained by applying the BET method[30] to the adsorption branch of the adsorption/desorption isotherm), mean pore size and cumulative pore volume (obtained by analysis of the desorption branch using the BJH[31,32] calculation method) are summarized in Table 3; pore size distributions are shown in Fig. 11.

Table 3 Textural parameters determined by N_2 adsorption/desorption measurements for materials **P1-P4**

	SSA (m^2/g)	Mean Pore Size (nm)	Cumulative Pore Volume (cm^3/g)
P1	8.1 ± 0.8	3.9 ± 0.4	0.026 ± 0.002
P2	7.8 ± 0.8	3.5 ± 0.4	0.022 ± 0.002
P3	6.5 ± 0.7	2.7 ± 0.3	0.018 ± 0.002
P4	3.2 ± 0.3	1.9 ± 0.2	0.009 ± 0.002

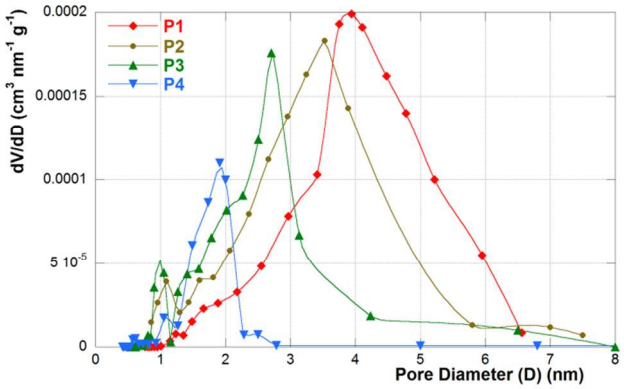

Fig. 11 Pore size distributions for materials **P1-P4**

All the samples show the typical adsorption/desorption isotherms for low porosity solids, which are characterized by the lack of any evident hysteresis loop, as well as by surface area values smaller than 10 m^2/g (the curve for **P2** is reported in Supporting as a representative example, Fig. S11). In particular, the almost complete lack of a hysteresis loop is consistent with the presence of cone-shaped pores,[32] which is typical for cyclodextrins. Inspection of data in Table 3 shows that the surface area and porous structure values regularly decrease on decreasing the **CD**/**C*n*** ratio, while pore distributions change accordingly. The observed trend accounts for the idea that the overall structure becomes more compact and the network less porous, because of the smaller dimensions of the calixarene units with respect to the cyclodextrin units. However, we can easily notice the sudden decrease in the values of all parameters, on passing from **P3** to **P4**. This behavior suggests that the overall hyper-reticulated structure undergoes a sort of contraction as the amount of the smaller co-monomer exceeds a critical value. This may have significant consequences on the possible sequestering abilities of the material (see later). Noticeably, the pore sizes are anyhow larger than the average **CD** annulus, even for material **P4**. Owing to the large relative uncertainties on the parameters values, we did not consider the opportunity to extend this study to materials **P5** and **P6**.

Absorption/sequestering tests

In order to assess the potential applications as nanosponges of our new co-polymer materials, we performed some tests to verify their abilities in absorbing/sequestering various organic guest molecules, selected as possible model pollutants or drugs, from an aqueous solution. We chose a set of nitroarenes, namely *p*-nitroaniline derivatives **5-8** and nitrobenzene **9**, together with some commercial dyes **10-13** (Scheme 4). It has been widely shown that *p*-nitroaniline derivatives interact effectively with **CD**s.[15,16] The study of the binding properties of both native and modified **CD**s towards this class of compounds has allowed to gain detailed information on the microscopic aspects of the inclusion process in solution. Noticeably, we designed *ad hoc* and synthesized compound **8** (as *p*-toluensulfonate salt) in such a way to possess at the same time also an imidazolium cationic moiety, potentially apt for inclusion in **C*n***s. On the other hand, nitrobenzene **9** was chosen because it is poorly included in **CD**s[33] but shows a fair affinity for **C*n***s.[34] Dyes **10-13** present diverse

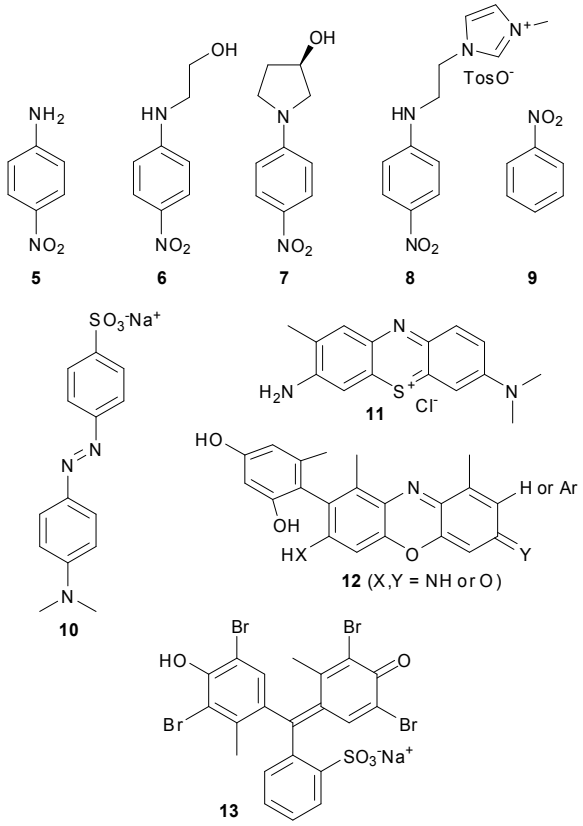

Scheme 4 Structures of model guests **5-13**.

structures and different charge, but share as a common feature the presence of a large, quite rigid conjugate framework. Methylorange **10** has been proven to have a good affinity for **CD**s[35] depending on the pH of the solvent medium, and therefore it is particularly suitable to test our materials under different pH conditions. Differently, cationic Toluidine Blue **11** (a phenothiazine derivative), neutral Orceine **12** (a complex mixture of structurally interrelated phenoxazines) and anionic Chresol Green **13** (a triphenylmethane derivative) were tested under neutral conditions only.

In order to carry out absorption tests, materials **P1-P6** were preliminarly grinded in a mortar and passed through a 200 μm sieve for having a rough control of particle size. In a typical test (see Experimental) we placed into a vial a carefully weighed amount of the powdered material with an aliquot of a solution of the model guest. The vial was mechanically shaken for 90 min (long enough to reach equilibrium). Then, the liquor was rapidly filtered and analyzed by UV-vis spectrophotometry, in order to determine the percent amounts of substance left in solution and sequestered by the polymer. Results are collected in Table 4.

Table 4 Absorption/sequestering tests.[a]

	5	**6**	**7**	**8**	**9**	**10** pH 2	**10** pH 8	**11**	**12**	**13**
P1	98	79	94	48	80	92	77	99	62	16
P2	85	73	91	42	74	95	73	99	65	15
P3	72.	72	89	32	69	96	65	98	65	13
P4	66	61	79	22	69	77	25	58	41	5
P5	59	46	67	13	73	57	17	51	34	5
P6	51	38	67	17	73	47	17	66	40	6

[a] All data are given within a ±2% indetermination.

As we can easily see, all the materials are able to absorb the model compounds, although their efficiencies show large variations depending on the guest. The best performances are generally shown by material **P1** (with the only exception of guest **10** at pH 2), which is able to sequester almost completely (> 98 %) *p*-nitroaniline **5** and Toluidine Blue **11** from the solution. Considering in particular *p*-nitroanilines **5**-**8**, absorption abilities towards these guests just decrease along the series of materials **P1**-**P6**, consistently with the decrease in the amount of the **CD** component present in the co-polymer. This indicates a larger affinity of these guests towards the **CD** rather than the C***n*** host cavity. In general, affinities seem to decrease along the series **7** > **5** > **6** > **8**, apparently according to the hydrophobic character of the guest. It is worth noting that this sequence does not match the trend for the relevant binding constants *K* with native **β-CD** in aqueous solution (namely 380 ± 40 M^{-1} for **5**,[33] 610 ± 30 M^{-1} for **6**,[16] 960 ± 20 M^{-1} for **7**,[16] 1530 ± 100 M^{-1} for **8**). As we already mentioned, binding constants in solution have been proven to be affected by a subtle balance between different microscopic factors,[14-16] which is critically controlled by the well known "induced fit" effect[36] allowed by the fair flexibility of the macrocycle. By contrast, absorption data account for a quite different situation, because the **CD** units embedded within the polymeric network should experience severe conformational restraints; consequently, hydrophobic effects may assume a major role. An interesting behavior is observed with derivative **8**. As a matter of fact, despite its *ad hoc* designed structure, our materials showed a modest affinity for it, probably because of its ionic nature making it quite hydrophilic. However, observed absorptions pass through a minimum from material **P1** to **P5**, and rise slightly on passing to **P6**, *i.e.* on increasing the amount of C***n*** units present in the polymer. This finding suggests that the C***n*** units do actually interact with the guest, presumably through its imidazolium moiety. Finally, it is interesting to notice that all the materials are able to absorb nitrobenzene **9** at an appreciable extent, with nearly negligible differences among them, despite it is poorly included in native **β-CD** ($K = 40 \pm 10$ M^{-1}).[33] Therefore, we may conclude that both the **CD** and the C***n*** units in the co-polymers show comparable affinities towards this particular guest and co-operate in its absorption.

On passing to analyze the results for dyes **10**-**13**, we can notice that the behavior shown by towards Methylorange **10** appears quite peculiar. As a matter of fact, the affinity of the materials towards the protonated form at pH 2 raises slightly on passing from **P1** to **P3**, and then falls down for the other polymers. By contrast, the behavior towards the anionic form (at pH 8) has a decreasing trend similar to the one shown towards *p*-nitroanilines. Noticeably, the protonated zwitterionic form of **10** is absorbed much more efficiently that the anionic one. So, once again the results suggest that absorption seems affected by the hydrophilic character of the substrate, as a function of its charge status. However, this is not the only factor involved. As a matter of fact, if we extend our consideration to the entire set, we can easily notice that cationic Toluidine Blue **11** is as much effectively sequestered as zwitterionic **10**, and more than anionic **10** or neutral Orceine **12**; on the other hand, the inclusion of anionic Chresole Green **13** is poor in all cases. Examining more in detail the whole of the results, we can easily notice a significant sudden drop in the absorption abilities on passing from **P3** to **P4**. Keeping in mind the fact that dyes **10**-**13** possess a large rigid framework, this observation perfectly parallels the fact that the porosity of the materials undergoes a drop for **P4**, as discussed previously. Furthermore, it is also interesting to notice that, as well as for the cationic *p*-nitroaniline imidazolium derivative **8**, polymer **P6** shows better sequestering abilities than **P5** towards guests **11** and **12**. Once again, this finding accounts for the fact that the C***n*** units play an active role as hosts, and thus cannot be considered as mere linkers between the **CD** units.

Finally, a few complementary tests were carried out with materials **P1** and **P3** and *p*-nitroanilines **5** and **7**. Negligible absorptions were observed as the guests were dissolved in common organic solvents such as methanol, ethanol, diethyl ether or ethyl acetate. On the other hand, after having been used in absorption tests, the materials could be easily recovered and regenerated by "washing" them one or, at worst, two times with a small amount of methanol.

Conclusions

Exploiting the CuAAC azide-alkyne 1,3-dipolar cycloaddition reaction, we were able to accomplish the synthesis of new **CD**-C***n*** co-polymers having different compositions. These materials were characterized by combined FT-IR, TGA/DTG, CP-MAS NMR and N_2 absorption/desorption techniques, which evidenced in particular their quantitative composition, thermal stability and low porosity texture. It is important to stress that the formation of the polymeric network takes place even if one of the co-monomers is present in large excess in the reaction mixture, although part of the excess component obviously remains unreacted, and therefore is lost during the work-up procedure.

Our materials possess all the features requested for a new class of nanosponges. Indeed, tests positively point out the actual ability of our materials to sequester organic molecules from an aqueous solution. These abilities undoubtedly depend on the composition of the material. In several cases, such as for *p*-nitroaniline derivatives which are effectively bound by **β-CD**, the affinity of the organic guest molecule for the polymer decreases on decreasing the amount of the **CD** component. However, affinities of the guests seem critically influenced by their hydrophobic character, and cannot be directly correlated with *K* values in solution. Probably, at least with some guests such as **9**, **11** and **12**, the **CD** and C***n*** moieties may act synergistically. Therefore, C***n*** units seem actually participating in the absorption process, and thus cannot be considered as mere linkers between the **CD** units. Finally, molecular dimensions as compared to the porosity of the materials may play an important role too, whenever large guest molecules are concerned.

Experimental

All the reagents and materials needed were used as purchased, with no further purification. Commercial **β-CD** hydrate was dried under vacuum at 90 °C overnight before use. The *heptakis*-(6-deoxy)-(6-iodo)-β-**CD**,[23] the *heptakis*-(6-azido)-(6-iodo)-β-**CD** **1**[58] and (5,11,17,23-tetra-*tert*-butyl)-(25,26,27,28-tetra-propargyl-oxy)-calix-[4]-arene **2**[22] were prepared and characterized

according to literature reports, as well as guests **6** and **7**.[15] Guest **8** was prepared from **6** *via* a two-step procedure. In particular, **6** was first converted into its *p*-toluen-sulfonyl ester, and the product obtained was then subjected to a simple nucleophilic displacement reaction with 1-methyl-imidazole.

FT-IR spectra were recorded on a JASCO 420 spectrometer. TGA-DTG experiments were performed on a Q5000 TA Instruments apparatus, heating each sample under a continuous nitrogen stream (25 mL/min) from 100 °C to 900°C with a 2.5 °C/min heating rate; each sample was equilibrated at 100 °C for a few minutes in the apparatus before the experiment. NMR spectra in solution were acquired on a Brucker AS Series 250 MHz instrument, whereas ^{13}C {^{1}H} CP-MAS spectra were acquired on a Brucker Avance II 400 MHz instrument, equipped with a 15 kHz rotating MAS probe. SSA measurements and pore texture analyses were performed using a Sorptomatic 1900 Carlo Erba Instrument, by physical adsorption/desorption of N_2 at the temperature of liquid nitrogen (-196 °C). The specific surface area was calculated by applying the BET method to the adsorption branch of the isotherm in the standard pressure range of 0.05-0.30 p/p0.[30] By analysis of the desorption branch, using the BJH calculation method in the range 0.42< p/p0<0.98, the pore size distribution and pore volume were also obtained.[31,32] The binding constant (at 298 K) between native **β-CD** and guest **8** was obtained by means of polarimetric measurements using a JASCO P-1010 polarimeter, according to the procedure described elsewhere.[37]

***heptakis*-(6-Deoxy)-(6-{[4-(*p*-*tert*-butylphenoxy)methyl]-1,2,3-triazol-1-yl})-β-CD 4**: compound **1** (131 mg, 0.10 mmoles), *p*-(*tert*-butyl)phenyl-propargyl ether **3** (411 mg, 2.1 mmoles), $CuSO_4{\cdot}5H_2O$ (40 mg, 0.16 mmoles) and sodium ascorbate (62 mg, 0.32 mmoles) were placed in a dark vial and dissolved/suspended in 4 mL of DMSO. The mixture was allowed to react overnight at 70 °C under magnetic stirring. Then the reaction mixture was poured into 70 mL of water, and the product was isolated by centrifugation, washed repeatedly with methanol and finally collected by filtration. Yield 90% (236 mg, 0.09 mmoles). Brown solid, decomposes before melting. FT-IR (nujol): see text. ^{1}H NMR (DMSO-d_6): δ_H = 1.19 (63 H, s, CH_3), 3.74 (7 H, m, **CD**-H(3)), 4.04 (7 H, m, **CD**-H(6)), 4.27 (7 H, m, **CD**-H(5)), 4.37 (7 H, m, **CD**-H(6')), 4.83 (14 H, br s, OCH_2), 5.16 (7 H, br s, **CD**-H(1)), 5.95 (7 H, bs s, **CD**-OH(3)), 6.07 (7 H, d, J = 5.0 Hz, **CD**-OH(2)), 6.80, 7.19 (14 H + 14 H, 2 d, J = 7.0 Hz, C_6H_4), 8.10 (7 H, s, triazole-H(5)); overlapped resonances for the **CD**-H(2) and **CD**-H(4) at ca. 3.39 ppm are covered by the signal due to residual water (see Fig. S7 in Supporting). ^{13}C NMR: δ_C = 31.2 (*t*Bu CH_3), 33.6 (*t*Bu C_{quat}), 55.3 (**CD**-C(6)), 60.8 (OCH_2), 71.7 (**CD**-C(2)), 72.3 (**CD**-C(3)), 77.9 (**CD**-C(5)), 82.7 (**CD**-C(4)), 101.6 (**CD**-C(1)), 113.9 , 125.8, 142.8, 155.7 (C_6H_4), 114.3 (triazole-C(5)), 142.6 (triazole-C(4)) (see Fig. S8 in Supporting). Element. anal. found C 60.77, H 6.74, N 21.28; $C_{133}H_{175}N_{21}$ requires C 60.79, H 6.71, N 21.31.

2-[*N*-(*p*-Nitrophenyl)-amino]-ethanol *p*-toluensulfonyl ester: compound **6** (3.64 g, 20 mmoles) was dissolved in 20 mL of dry pyridine at 0 °C, and to the solution *p*-toluen-sulfonyl chloride (4.76 g, 25 mmoles) was added in small portions. The system was then allowed to warm up to r.t. and kept overnight under magnetic stirring. The reaction mixture was then poured into 200 mL of water and the crude product filtered off, washed repeatedly with aqueous 0.1 M HCl, and finally crystallized from methanol. Yield 83 % (5.58 g). Yellow crystals; m.p. 124-126 °C. FT-IR (nujol, cm^{-1}): 3408, 1604, 1462, 1306, 1291. ^{1}H-NMR (DMSO-d_6): δ_H = 2.26 (3H, s, CH_3), 3.17, 3.51 (2 H + 2 H, 2 t, J = 5.7 Hz, CH_2-CH_2), 4.04 (1 H, br s, NH), 6.50 and 7.91 (2 H + 2 H, 2 d, J = 7.4 Hz, $NO_2C_6H_4$), 7.23, 7.56 (2 H + 2 H, 2 d, J = 8.2 Hz, tosylate). Element. anal. found C 53.58, H 4.78, N 8.34; S 9.50; $C_{15}H_{16}N_2O_5S$ requires C 53.56, H 4.79, N 8.33, S 9.53.

1-[2-*N*-(*p*-Nitrophenyl)-aminoethtyl]-3-methyl-imidazolium *p*-toluensulfonate salt 8: 2-[*N*-(*p*-Nitrophenyl)-amino]-ethanol *p*-toluen-sulfonyl ester (1.68 g, 5 mmoles) and 1-methyl-imidazole (2 mL, 2.43 g, 29.6 mmoles) were dissolved in 10 mL of ethanol and allowed to react at 60 °C for 24 h. The reaction mixture was then dropped under vigorous stirring into 150 mL of ethyl acetate, and the precipitated product was filtered off (no further purification was needed). Yield 44% (0.91 g). Yellow crystals, m.p. 140-142 °C. IR (nujol, cm^{-1}): 3424, 1606, 1464. ^{1}H-NMR (DMSO-d_6): δ_H 2.34 (3H, s, CH_3(tosilate)), 3.70 (2 H, m, CH_2), 3.88 (1 H, s, CH_3(imidazolium)), 4.41 (2 H, t, J = 5.6 Hz, CH_2(imidazolium)), 6.75 and 8.05 (2 H + 2 H, 2 d, J = 9.1 Hz, *p*-$NO_2C_6H_4$), 7.18 and 7.56 (2 H + 2 H, 2 d, J = 8.0 Hz, tosylate), 7.44 (1 H, t, J = 5.9 Hz, NH) 7.56 (1 H, s, H(imidazolium)), 7.84 (1 H, s, H(imidazolium)), 9.18 (1 H, s, H(imidazolium)) (see Fig. S9 in Supporting). ^{13}C-NMR (DMSO-d_6): δ_C 20.7 (CH_3(tosylate)), 35.6 (CH_3 (imidazolium)), 42.0 (CH_2 (imidazolium)), 47.8 (CH_2), 111.1, 125.4, 136.4 and 153.9 (*p*$NO_2C_6H_4$), 112.4, 123.5, 137.0 (imidazolium), 126.0, 128.0, 137.7, 145.5 (C_6H_4(tosylate)) (see Fig. S10 in Supporting). Element. anal. found C 54.51, H 5.34, N 13.38, S 7.62; $C_{19}H_{22}N_4O_5S$ requires C 54.53, H 5.30, N 13.39, S 7.66.

***Synthesis of materials P1-P6* -** The proper amounts of the co-monomers **1** and **2** (as specified in Table 1) were mixed in a dark vial together with $CuSO_4{\cdot}5H_2O$ (40 mg, 0.16 mmoles) and sodium ascorbate (62 mg, 0.32 mmoles). Then 4 mL of DMSO were added and the solution/suspension was allowed to react overnight at 70 °C under magnetic stirring. The isolation of the polymeric product was carried out according to three different washing protocols. *i*) The reaction mixture was first poured into 50 mL of water, subjected to sonication in an ultrasound bath for 15 min and centrifugated; the solid residue was then suspended in 50 mL of methanol, sonicated again and centrifugated; this suspension-sonication-centrifugation sequence was repeated two more times, the first one with another portion of methanol and the second one with 50 mL of diethyl ether; finally, the solid residue was filtered off and dried in vacuo at 60 °C for two hours. *ii*) The reaction mixture was first poured into 50 mL of methanol, and then subjected to a procedure similar to the one described above, washing afterwards in sequence with water, then methanol again and finally diethylether; the filtered product was eventually dried in vacuo at 60 °C for two hours. *iii*) The reaction mixture was first poured into 50 mL of diethylether, and then subjected to the aforementioned procedure, washing afterwards in sequence with methanol, then water and finally methanol again; the filtered product was dried in vacuo at 60 °C for three hours.

Absorption/sequestering and recovering tests - A carefully weighed amount (4.0 mg) of the powdered material was placed into a vial with an aliquot (2 mL) of a mother solution of the

model guest ($1 \cdot 10^{-4}$ M for guests **5-9**, $5 \cdot 10^{-5}$ M for guests **10-13**). The vial was shaken for 90 min using the mechanic device of a common Parr hydrogenation apparatus; then the liquor was rapidly filtered through a 0.45 μM Millipore filter, and analyzed. After the absorption tests, the material was recovered and placed in a vial with methanol (5 mL); the suspension was sonicated for 5 min and filtered. The procedure was repeated one or two more times, until the filtrate showed negligible UV-vis absorption.

Acknowledgments

CP-MAS NMR experiments were recorded at the *Centro Grandi Apparecchiature - UniNetLab - Università di Palermo* funded by *P.O.R. Sicilia 2000-2006, Misura 3.15 Quota Regionale*; Dr. A. Spinella is gratefully aknowledged for useful suggestions and discussion.

Notes and references

[a] *Dipartimento STEBICEF, University of Palermo,V.le delle Scienze, pad. 17, 90128 - Palermo,Italy. Fax: +39 091 596825; Tel: +39 091 23879537; E-mail: paolo.lomeo@unipa.it, renato.noto@unipa.it.*
[b] *Dipartimento di Fisica e Chimica, University of Palermo,V.le delle Scienze, pad. 17, 90128 - Palermo,Italy.. Fax: +39 091 590015; Tel: +39 091 23897962; E-mail: giuseppe.lazzara@unipa.it.*
[b] *ISMN-CNR Palermo, via Ugo La Malfa 153, 90128 - Palermo, Italy. Fax: +39 091 6809399; Tel: +39 091 6809371; E-mail: leonarda.liotta@pa.ismn.cnr.it.*

† Electronic Supplementary Information (ESI) available: ^{1}H and ^{13}C NMR spectra of compounds 4 and 8; FT-IR spectra of materials **P1**-**P6**; N_2 adsorption desorption isotherm of material **P2**; a short discussion on quantitative NMR data processing. See DOI: 10.1039/b000000x/

1 (a) F. Trotta, W. Tumiatti, Pat. Wo 03/085002, **2003**. (b) R. Cavalli, F. Trotta, W. Tumiatti, *J. Incl. Phenom. Macrocycl. Chem*., 2006, **56**, 209-213. (c) F. Trotta, R. Cavalli, *Compos. Interface,* 2009, **16**, 39-48. (c) S. Subramanian, A. Singireddy, K. Krishnamoorthy, M Rajappan, *J. Pharm. Pharm. Sci.,* 2012, **15**, 103-111.

2 (a) F. Trotta, M. Zanetti, R. Cavalli, *Beilstein J. Org. Chem*. 2012, **8**, 2091. (b) A. Vyas, S. Saraf, S. Saraf, *J. Incl. Phenom. Macrocycl. Chem.* 2008, **62**, 23-42. (c) S. Swaminathan, P. R. Vavia, F. Trotta, R. Cavalli, S. Tumbiolo, L. Bertinetti, S. Coluccia, *J. Incl. Phenom. Macrocycl. Chem.* 2013, **76**, 201-211.

3 (a) L. Seglie, D. Spadaro, F. Trotta, M. Devecchi, M. L. Gullino, V. Scariot, *Posthaverest Biol. Technol*. 2012, **64**, 55-57. (b) L. Seglie, K. Martina, M. Devecchi, C. Roggero, F. Trotta, V. Scariot, *Posthaverest Biol. Technol*. 2011, **59**, 200-205. (c) L. Seglie, K. Martina, M. Devecchi, C. Roggero, F. Trotta, V. Scariot, *Plant Growth Regul*. 2011, **65**, 505-511.

4 (a) F. Trotta, R. Cavalli, K. Martina, M. Biasizzo, J. Vitillo, S. Bordiga, P. Vavia, K. Ansari, *J. Incl. Phenom. Macrocycl. Chem.* 2011, **71**, 189-194. (b) R. Cavalli, A. K. Akhter, A. Bisazza, P. Giustetto, F. Trotta, P. Vavia, *Int. J. Pharm.* 2010, **402**, 254-257. (c) M. Schlichtenmayer, M. Hirscher, *J. Mater. Chem.* 2012, **22**, 10134-10143.

5 (a) B. B. Mamba, R. W. Krause, T. J. Malefetse, G. Gericke, S. P. Sithole, *J. Water Suppl. Res. T.* 2009, **58**, 299-304. (b) D. P. Hashim, N. T. Narayanan, J. M. Romo-Herrera, D. A. Cullen, M. G. Hahm, P. Lezzi, J. R. Suttle, D. Kelkhoff, E. Muñoz-Sandoval, S. Ganguli, A. K. Roy, D. J. Smith, R. Vajtai, B. G. Sumpter, V. Meunier, H. Terrones, M. Terrones, P. M. Ajayan, *Sci. Rep.* 2012, **2:363**, 1-8. (c) B. B. Mumba, R. W. Krause, T. J. Malefetse, E. N. Nxumalo, *Envirom. Chem. Lett.* 2007, **5**, 79-84. (d) S. H. Mhlongo, B. B. Mamba, R. W. Krause, *Phys. Chem. Earth* 2009, **34**, 819-824.

6 A. M. Layre, N. M. Gosselet, E. Renard, B. Sebille, C. Amiel, *J. Incl. Phenom. Macrocycl. Chem.* 2002, **43**, 311-317.

7 (a) J. Alongi, M. Pošković, A. Frache, F. Trotta, *Polym. Degrad. Stabil.* 2010, **95**, 2093-2100. (b) F. Trotta, P. Ferruti, E. Ranucci, M. Veglia, C. Baggiani, C. Giovannoli, *J. Incl, Phenom. Macrocycl. Chem*. 2007, **57**, 657-661. (c) M. H. Mohamed, L. D. Wilson, D. Y. Pratt, R. Guo, C. Wu, J. D. Headley, *Carbohyd. Polym.* 2012, **87**, 1241-1248. (d) S. Berto, M. C. Bruzzaniti, R. Cavalli, D. Perrachon, E. Prenesti, F. Trotta, C. Sarzanini, W. Tumiatti, *J. Incl. Phenom. Macrocycl. Chem*. 2007, **57**, 631-636.

8 F. Castiglione, V. Crupi, D. Majolino, A. Mele, W. Panzeri, B. Rossi, F. Trotta, V. Venuti, *J. Incl. Phenom. Macrocycl. Chem.* 2013, **75**, 247-254.

9 M. Ma, D. Q. Li, *Chem. Mater.* 1999, **11**, 872-874.

10 (a) L. D. Wilson, M. H. Mohamed, J. V. Headley *J. Colloid Interf. Sci.* 2011, **357**, 215-222. (b) A. H. Karoyo, L. D. Wilson *J. Colloid Interf. Sci.* 2013, **402**, 215-222.

11 (a) A. Ikeda, S. Shinkai, *Chem. Rev.* 1997, **97**, 1713-1734. (b) C. D. Gutsche, B. Dhawan, K. H. No, R. Muthukrishnan, *J. Am. Chem. Soc.* 1981, ***103***, 3782-3792. (c) C. D. Gutsche, L.-G. Lin, *Tetrahedron* 1986, ***42***, 1633-1640. (d) C. D. Gutsche, J. A. Levine, *J. Org. Chem*. 1985, ***50***, 5802-5806. (e) J. D. Van Loon, A. Arduini, L. Coppi, W. Verboom, A. Pochini, R. Ungaro, S. Harkema, D. N. Reinhoudt, *J. Org. Chem.* 1990, ***55***, 5639-5646.

12 (a) D. A. F. de Narmor, R. M. Cleverley, M. L. Zapata-Ormachea, *Chem. Rev*. 1998, ***98***, 2495-2525. (b) J. W. Steed, J. L. Atwood in *Supramolecular Chemistry*, ed. Wiley, New York, 2000, pp. 170-182. (c) E. A. Shokova, V. V. Kovalev, *Russ. J. Org. Chem*. 2009, **45**, 1275-1314.

13 H.-J. Schneider, *Angew. Chem. Int. Ed*. 2009, **48**, 3924-3977.

14 (a) K. A. Connors, *Chem. Rev*. 1997, **97**, 1325-1358. (b) M. V. Rekharsky, Y. Inoue, *Chem. Rev*. 1998, **98**, 1875-1918. (c) I. Tabushi, Y. Kiyosuke, T. Sugimoto, K. Yamamura, *J. Am. Chem. Soc.* 1978, **100**, 916-919. (d) I. Tabushi, T. Mitzutani, *Tetrahedron* 1987, **43**, 1439-1447. (e) L. Liu, Q.-X. Guo, *J. Inclusion Phenom. Macrocyclic Chem.* 2002, **42**, 1-14. (f) M. Wedig, S. Laug, T. Christians, M. Thunhorst, U. Holzgrabe, *J. Pharm. Biomed. Anal.* 2002, **27**, 531-540. (g) M. V. Rekharsky, Y. Inoue, *J. Am. Chem. Soc.* 2000, **122**, 4418-4435. (h) M. V. Rekharsky, Y. Inoue, *J. Am. Chem. Soc.* 2002, **124**, 813-826. (i) K. Kano, H. Hasegawa, *J. Am. Chem. Soc.* 2001, **123**, 10616-10627. (j) M. V. Rekharsky, M. P. Mayhew, R. N. Goldberg, P. D. Ross, Y. Yamashoji, Y. Inoue, *J. Phys. Chem. B* 1997, **101**, 87-100.

15 (a) P. Lo Meo, F. D'Anna, S. Riela, M. Gruttadauria, R. Noto, *Org. Biomol. Chem.* 2003, **1**, 1584-1590. (b) P. Lo Meo, F. D'Anna, M. Gruttadauria, S. Riela, R. Noto, *Tetrahedron* 2004, **60**, 9099-9111.

16 (a) P. Lo Meo, F. D'Anna, S. Riela, M. Gruttadauria, R. Noto, *Tetrahedron* 2009, **65**, 2037-2042. (b) P. Lo Meo, F. D'Anna, S. Riela, M. Gruttadauria, R. Noto, *J. Incl. Phenom. Macrocycl. Chem.* 2011, **71**, 121-127.

17 J. C. Ma, D. A. Dougherty, *Chem. Rev.* 1997, **97**, 1303-1324.

18 (a) W. Sliwa, T. Girek, *J. Incl. Phenom. Macrocycl. Chem.* 2010, **66**, 15-41. (b) R. M. Izatt, K. Pawlak, J. S. Bradshaw, R. L. Bruening, *Chem. Rev.* 1991, **91**, 1721-2085. (c) R. M. Izatt, K. Pawlak, J. S. Bradshaw, R. L. Bruening, B. J. Tarbet *Chem. Rev.* 1992, ***92***, 1261-1354. (d) R. M.; Izatt, K.; Pawlak, J. S. Bradshaw, *Chem. Rev.* 1995, ***95***, 2529-2586. (e) F. Tancini, T. Gottschalk, W. B. Schweitzer, F. Diedrich, E. Dalcanale, Cem. Eur. J. 2010, **16**, 7813-7819.

19 (a) L. Li, H. Y. Zhang, Y. Liu, *Sci. Chin. Chem.* 2012, **55**, 1092-1096. (b) X. Zhang, L. Shi, G. Xu, C. Chen, *J. Incl. Phenom. Macocycl. Chem.* 2013, **75**, 147-153. (c) M. Tabatabai, H. Ritter, *Beilstein J. Org. Chem*. 2010, **6**, 784-788.

20 (a) R. Huisgen, in *1,3-Dipolar Cycloaddition Chemistry*; (Ed. A. Padwa) Wiley, New York, 1984, pp. 1-176. (b) C. W. Tornøe, C. Christensen, M. Meldal, *J. Org. Chem*. 2002, **67**, 3057-3064. (c) V. V. Rostoftzef, L. G. Green, V. V. Forkin, K. B. Sharpless, *Angew. Chem. Int. Ed.* 2002, **41**, 2596-2599. (d) M. Meldal, C. W. Tornøe, *Chem. Rev*. 2008, **108**, 2952-3015.

21 Z. Szurmai, A. Liptak, J. Szejtli, *Starch-Stärke* 1990, **42**, 447-449.

22 M. J. Chetcuti, A. M. J. Devoille, B. Othman, R. Souane, P. Thuery, J. Vicens, *Dalton Trans.* 2009, 2999-3008.

23 B. I. Gorin, R. J. Riopelle, G. R. J. Thatcher, *Tetrahedron Lett.* 1996, **37**, 4647-4650.

24 (a) H. Staudinger, J. Meyer, *Helv. Chim. Acta* 1919, **2**, 635-646. (b) W. Tagaki, K. Yano, K. Yamanaka, H. Yamamoto, T. Miyasaka, *Tetrahedron Lett.* 1990, **31**, 3897-3900.

25 (a) F. Castiglione, V. Crupi, D. Majolino, A. Mele, B. Rossi, F. Trotta, V. Venuti, *J. Phys. Chem. B* 2012, **116**, 7952-7958. (b) A. Mele, F. Castiglione, L. Malpezzi, F. Ganazzoli, G. Raffaini, F. Trotta, B. Rossi, A. Fontana, G. Giunchi, *J. Incl. Phenom. Macrocycl. Chem.* 2011, **69**, 403-409.

26 (a) S. Riela, G. Lazzara, P. Lo Meo, S. Guernelli, F. D'Anna, S. Milioto, R. Noto, *Supramol. Chem*. 2011, **23**, 819-828. (b) Y. Bai, J. Wang, M. Bashari, X. Hu, T. Feng, X. Xu, Z. Jin, Y. Tian *Thermochim. Acta* 2012, **541**, 62-69.

27 (a) D. D. Laws, H.-M. L. Bitter, A. Jerschov, *Angew. Chem. Int. Ed.* 2002, **41**, 3096-3129. (b) M. J. Gidley, S. M. Bociek, *J. Am. Chem. Soc.* 1988, **110**, 3820-3829. (c) W. G. Blann, C. A. Fyfe, J. R. Leyrla, C. S. Yannoni, *J. Am. Chem. Soc.* 1981, **103**, 4030-4033.

28 (a) P. T. Larsson, E.-L. Hult, K. Wickholm, E. Pettersson, T. Iversen, *Solid State Nucl. Magn. Res.* 1999, **15**, 31-40. (b) P. Conte, A. Piccolo, B. van Lagen, P. Buurman, M. A. Hemminga, *Solid State Nucl. Magn. Res.* 2002, **21**, 158-170.

29 (a) L. Shao, C. Mu, H. Du, Z. Czech, H. Du, Y. Bai *Appl. Surf. Sci.* 2011, **258**, 1682-1688. (b) G. Mamba, X. Y. Mbianda, P. P. Govender, *Carbohyd. Polym.* 2013, **98**, 470-476.

30 S. J. Gregg, K. S. Sing, *Adsorption, Surface Area and Porosity* , ed. Academic Press, San Diego, 2nd edn. 1982.

31 S. Brunauer, P.H. Emmet, E. Teller, *J. Am. Chem. Soc*. 1938, **60**, 309-319.

32 E. P. Barret, L. G. Joyner, P.P. Halenda, *J. Am. Chem. Soc.* 1953, 73, 373-380.

33 F. D'Anna, P. Lo Meo, S. Riela, M. Gruttadauria, R. Noto, *Tetrahedron*, 2001, **57**, 6823-6827.

34 E. B. Brouwer, G. B. Enright, J. A. Ripmeester, *Supamol. Chem*. 1996, **7**, 7-9.

35 H.-J. Buschmann, E. Schollmeyer, *J. Incl, Phenom. Macrocycl. Chem*. 1997, **29**, 167-174.

36 Rekharsky, M. V.; Yamamura, H.; Kawai, M.; Inoue, I. *J. Org. Chem.* 2003, **68**, 5228-5235.

37 (a) P. Lo Meo, S. Riela, F. D'Anna, M. Gruttadauria, R. Noto, *Tetrahedron Lett.* 2006, **60**, 9099-9102. (b) P. Lo Meo, F. D'Anna, S. Riela, M. Gruttadauria, R. Noto, *Tetrahedron* 2007, **63**, 9163-9171.

Cyclodextrin-calixarene co-polymers as a new class of nanosponges

Paolo Lo Meo,*[a] Giuseppe Lazzara,[b] Leonarda Liotta,[c] Serena Riela[a] and Renato Noto*[a]

Graphical Abstract

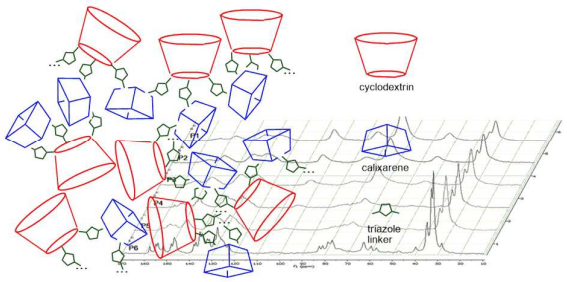

Novel nanosponge materials, obtained by co-polymerization of cyclodextrin and calixarene derivatives, have been characterized by various techniques and tested for removal of model pollutants from aqueous solution.